JOURNAL OF MATERIALS SCIENCE LETTERS 16 (1997) 23–26

Stress-rupture of continuous fibre ceramic composites at intermediate temperatures

E. LARA-CURZIO, M. K. FERBER
Metals and Ceramics Division, Oak Ridge National Laboratory, Oak Ridge, TN 37831 USA

Because of their potential to retain strength and to exhibit tough behaviour, continuous fibre-reinforced ceramic composites (CFCCs) are considered candidate materials for several applications at temperatures above 1000 °C. The driving force behind the development of these materials is the promise of substantial economic and environmental benefits if they are used in defence, energy and related industrial technologies [1]. The selection of CFCCs for energy-related industrial applications, where component service lives are measured in the tens of thousands of hours, will be determined in great part by their durability and reliability under thermal and mechanical loading in harsh environments. Studies of the durability of CFCCs have consisted mainly of staged static oxidation experiments followed by mechanical evaluation at room temperature [2]. Often the behaviour of CFCCs at the intermediate temperatures has been ignored by assuming that the severity of the treatment is directly proportional to the test temperature.

Although the oxidation embrittlement of Nicalon^{TM}/glass-ceramics has been well documented over the temperature range 800–1000 °C [3], recent studies reveal that these CFCCs experience severe environmental degradation after ageing treatments in air at even lower temperatures [4]. The environmental degradation of these materials consists of loss of the carbonaceous fibre coating, oxidation of the fibres, filling of the spaces previously occupied by the carbon-fibre coating with silica and resulting loss of "ductility" and strength. These processes occur at temperatures where the environmental stability of CFCCs had not been considered an issue. For example, the ductile-to-brittle transformation temperature for Nicalon^{TM}/CAS has been found to be in the range 375–450 °C in air [4]. The micromechanical mechanisms that accompany the environmental degradation of these materials consist of increases in both the fibre bond strength and the fibre sliding resistance. At the same time, these mechanisms translate into substantial reductions in the average fibre pull-out length that would be observed on the fracture surfaces, and reductions of strength because of fibre damage. Although these studies have documented the severity of the environmental degradation even under static oxidation conditions, the decreases in fracture resistance and strength occur more rapidly under stress. The flexural stress-rupture behaviour of Nicalon^{TM}/SiC with a carbonaceous fibre coating in air has been studied at temperatures between 425 and 1150 °C [5]. It was found that the life of this material decreased exponentially with the maximum applied tensile stress and that there was a "static fatigue limit" of 100 MPa for test temperatures below 1000 °C. Furthermore, the presence of a seal coating at 425 °C was found to extend the life of the material by a factor of 10 with respect to unsealed specimens [5]. Although the significance of these results is very clear, the evaluation of the stress-rupture behaviour of two-dimensional CFCCs in flexure has the disadvantages that upon matrix cracking the state of stress in the specimen is very complex and that it will also change with time due to load redistribution. Furthermore, other processes, such as delamination, may occur and complicate the interpretation of the results. Evidently, for design purposes, it is necessary to evaluate this behaviour in tension.

This letter reports the tensile stress-rupture behaviour of Nicalon^{TM}/SiC in air at 425 °C and presents a qualitative model to explain the results. Dog bone-shaped specimens 200 mm long, 3.5 mm thick and 10.2 mm wide in the gauge section, were used. The tests were conducted in a universal testing machine equipped with a compact furnace that produced a uniformly heated zone of 30 mm along the gauge length of the specimen. The specimens had adhesively bonded aluminium end-tabs and were gripped using water-cooled hydraulically actuated grips. The material consisted of plain weave CG Nicalon^{TM} fibre fabric coated with a 0.3 μm thick layer of carbon. The SiC matrix was densified by chemical vapour infiltration and the samples had an external glassy seal coating of proprietary composition (BF Goodrich, Super-Temp Division, Santa Fe Springs, CA 90670). The specimens were heated at a uniform rate of 20 °C min^{-1} to the test temperature while maintaining a constant tensile load of 50 N in the load train. This was followed by a soaking period of 20 min to attain thermal equilibrium. The specimens were mechanically loaded at a constant rate of 10 N s^{-1} to the test load and then the load was maintained constant for the duration of the test, which was completed when the specimen failed. The longitudinal deformation of the specimen was monitored during the test using a low contact force capacitance extensometer with a gauge length of 25 mm.

Fig. 1 shows the strain history of the tensile stress-rupture tests at stresses of 100, 150 and 200 MPa. Based on acoustic emission data recorded

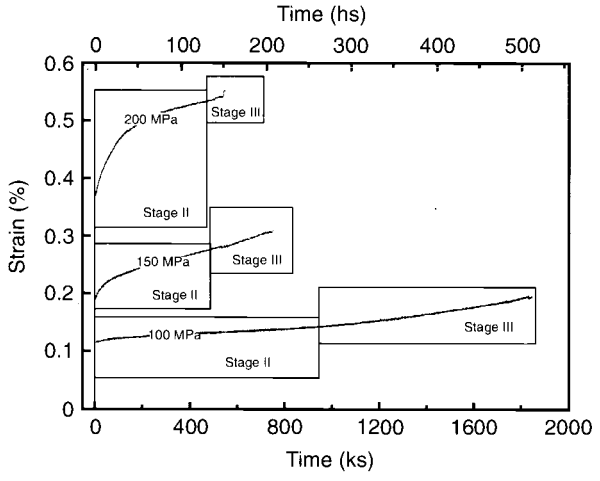

Figure 1 Plot of strain versus time curves for a Nicalon^{TM}/SiC CFCC at 425 °C in air at 100, 150 and 200 MPa.

during monotonic tensile tests at room temperature, it is assumed that substantial matrix cracking occurred during mechanical loading up to the test stresses. The strain versus time curves in Fig. 1 exhibit three well-defined regimes. Stage I coincides with the mechanical loading of the specimen. Stage II is characterized by a regime of decreasing rate of deformation, while in Stage III the rate of deformation increases leading to the failure of the specimen.

A qualitative model based on the simultaneous occurrence of thermo-chemical and micromechanical mechanisms at the fibre–matrix interface level is presented to explain the stress-rupture behaviour of the CFCC studied. According to this model, one mechanism dominates the rate of deformation in each one of the three stages that characterize the stress-rupture curves in Fig. 1. Fig. 2 schematically shows these mechanisms. In Stage I, matrix cracking, which is induced during mechanical loading, is accompanied by fibre debonding and sliding, with the debonded fibres effectively bridging the transverse cracks in the matrix. Stage II commences at the end of the monotonic loading when the carbonaceous fibre coating starts to oxidize. When the matrix cracks, the stress in the fibres at the plane of the crack increases to support the entire applied composite stress. Moving away from the crack surfaces, the average fibre stress decays linearly at a longitudinal rate of $2\tau/r$ as the matrix picks up the complementary portion of the load, where τ is the average interfacial shear stress and r the fibre radius. However, this mechanism is inhibited along those portions of the fibres that have lost physical contact with the matrix because of loss of the fibre coating by oxidation (Fig. 2). (This is different from fibre debonding when the fibre coating is still present. In the latter case, load transfer by shear between the fibres and the matrix and vice versa, is still possible through the fibre coating because of residual stresses and/or interface roughness). This complete decohesion of the fibres will result in subjecting longer portions of the fibres to the peak stress (σ/v_f) and also in an increase in the elongation of the specimen at a rate approximately given by

$$\frac{dx}{dt} \propto \frac{\sigma}{v_f E_f} \frac{dl_r}{dt} \tag{1}$$

where σ is the constant far-field tensile stress applied to the composite, v_f is the volume fraction of fibres in the longitudinal direction, E_f is the fibre elastic modulus and dl_r/dt is the rate of oxidation of the carbon interphase. As the supply of carbon decreases and as the access to the remaining carbon becomes more difficult, the rate of carbon oxidation will

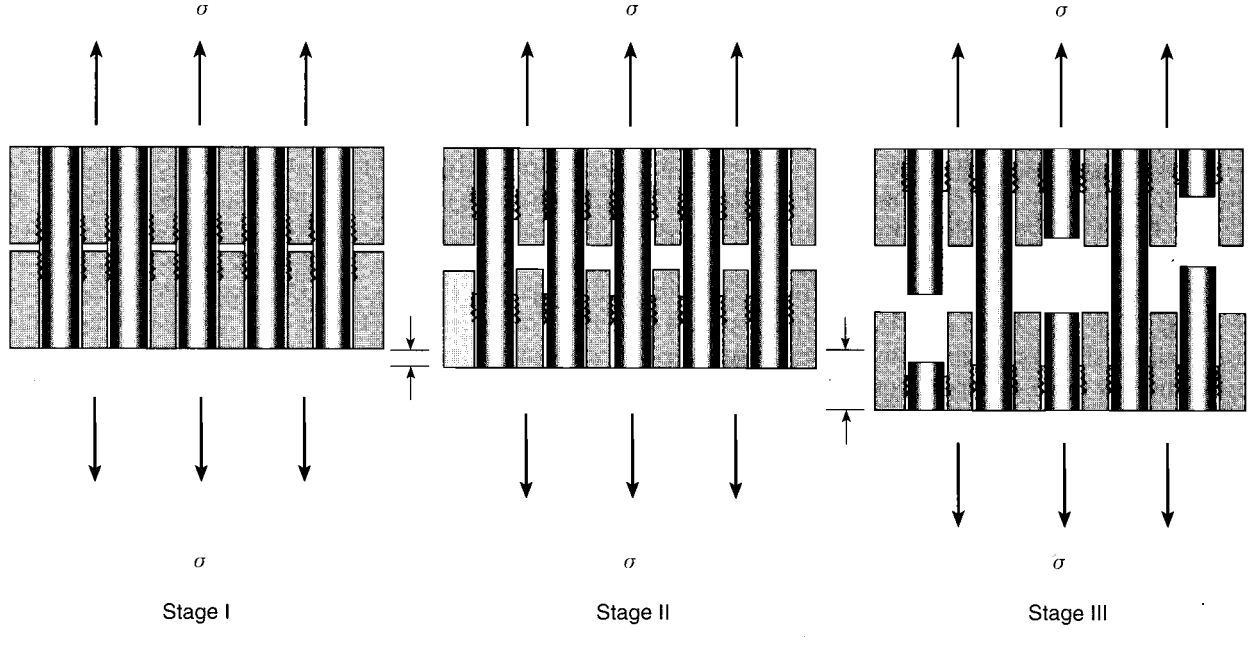

Figure 2 Schematic representation of the sequence of events responsible for the time-dependent deformation exhibited by the curves in Fig. 1. Stage I coincides with the monotonic loading of the specimen to the test stress. Stage II is associated with the burn-out of the carbon fibre coating and the decohesion of the fibre. This results in an increase in the specimen compliance at a decreasing rate that is controlled by the oxidation of carbon and the diffusion of gases along the channels between the fibres and the matrix. Stage III corresponds to a regime of progressive fibre failure in a domino effect fashion. This stage is characterized by an increase in the rate of deformation.

decrease, resulting also in the decreasing rate of deformation that characterizes Stage II.

In the absence of a fibre–matrix interface, global load-sharing conditions will prevail so that when fibres fail during the test, the load previously carried by those fibres will be transferred to the surviving fibres. By overloading the surviving fibres, their probability of failure will increase, hence generating a domino effect. In Stage III, the rate of elongation of the specimen will be dominated by progressive fibre failure and will be approximately given by

$$\frac{dx}{dt} \propto \frac{\sigma}{(1-\zeta)^2} \tag{2}$$

where ζ is the fraction of broken fibres. The increasing rate of deformation predicted by Equation 2 as a result of progressive fibre failure, is consistent with the accelerated deformation observed in Stage III of the strain versus time curves.

When plotting the maximum tensile stress versus time-to-failure as in Fig. 3 the results can be described by

$$t_f = A\sigma^{-n} \tag{3}$$

where $A = 4.282 \times 10^{-5}$, $n = 1.77$, σ is the tensile stress (MPa), and t_f is the life of the specimen (h). Statistical models of the time-dependent breakdown of fibres and fibre bundles indicate that although the lifetime of the bundle is shorter than the average lifetime of its component filaments under the same stress, the lifetimes of the bundle and the component filaments are scaled by the same breakdown rule [6, 7]. Therefore, it follows that the characteristic strength of the Nicalon™ fibres decreases with time in the manner predicted by Equation 3. Because it has been reported that even at 425 °C a layer of amorphous silica will form on the Nicalon™ fibre surface [8], it is postulated that this mechanism and the fact that the fibre length subjected to the peak stress increases with time are responsible for their strength degradation. Fractographic analysis of the fibres revealed that the fibres failed mostly from surface defects.

Fig. 4 shows a scanning electron micrograph of the fracture surface of the specimen that was tested at 150 MPa. This micrograph illustrates the magnitude of the fibre pull-out lengths which are several millimetres long. These extremely long fibre pull-out lengths are consistent with the sequence of mechanisms presented in Fig. 2 and are contrasted with fibre pull-out lengths of specimens that were fast fractured at room temperature which were of the order of hundreds of micrometres.

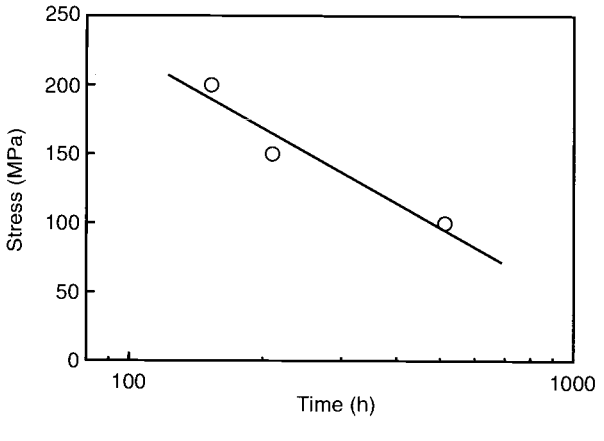

Figure 3 Plot of the stress versus time-to-failure for Nicalon™/SiC at 425 °C in air.

Figure 4 Scanning electron micrograph of the stress-ruptured specimen tested at 425 °C and 150 MPa. Notice the extremely long fibre pull-out lengths.

The results presented in this paper highlight two serious problems that could limit the performance of CFCCs: (i) the ineffectiveness of the external seal coating to protect the interior of the material at intermediate temperatures, and (ii) the time-dependent degradation of Nicalon™ fibres at relatively low temperatures. Although the design of many CFCCs incorporates the use of protective coatings, the mechanism responsible for the functionality of most of these coatings (e.g. formation of a protective oxide layer) is ineffective at intermediate temperatures due to the slow growth rate of the oxide product. Furthermore, although many designs will limit the use of CFCCs to stresses below the matrix cracking stress, it will still be necessary to determine their reliability when accidental stress excursions above the matrix cracking stress occur. In the light of the results presented in this letter, this evaluation will not need to be limited to the expected service temperatures, but should also include intermediate temperatures, because components will be exposed to this temperature regime during heating or cooling to/from the higher service temperatures.

Acknowledgements

This research was sponsored by the US Department of Energy, Assistant Secretary for Energy Efficiency and Renewable Energy, Office of Industrial Technologies, Industrial Energy Efficiency Division and Continuous Fiber Ceramic Composites Program and by the US Department of Energy, Assistant

Secretary for Energy Efficiency and Renewable Energy, Office of Transportation Technologies as Part of the High Temperature Materials Laboratory User Program under contract DE-AC05-96OR22464 with Lockheed Martin Energy Research Corporation. The authors thank Mr Stephan Russ for his dedicated work with the scanning electron microscope, and Peter F. Tortorelli, H.-T. Lin and K. Plucknett, Oak Ridge National Laboratory, for reviewing the manuscript and for stimulating discussions

References

1. M. A. KARNITZ, D. F. CRAIG and S. L. RICHLEN, *Ceram. Bull.* **70** (1991) 430.
2. P. F. TORTORELLI, L. RIESTER and R. A. LOWDEN, *Ceram. Eng. Sci. Proc.* **14** (1993) 358.
3. R. L. STEWART, K. CHYUNG, M. P. TAYLOR and R. F. COOPER, in "Fracture Mechanics of Ceramics Composites, Impact, Statistics and High-Temperature Phenomena", Vol. 7, edited by R. C. Bradt, A. G. Evans, D. P. H. Hasselman and F. F. Lange (Plenum Press, New York, 1985) pp. 33–51.
4. K. P. PLUCKNETT, R. L. CAIN and M. H. LEWIS, Materials Research Society Symposium Proceedings, Vol. 365, edited by R. A. Lowden, M. K. Ferber, J. R. Hellmann, K. K. Chawla and S. G. DiPietro (Materials Research Society, Pittsburg, PA, 1995) pp. 421–6.
5. H.-T. LIN, P. F. BECHER and P. F. TORTORELLI, *ibid.*, pp. 435–40.
6. B. D. COLEMAN, *J. Appl. Phys.* **29** (1958) 968.
7. E. LARA-CURZIO and M. K. FERBER, unpublished results (1996).
8. T. SHIMOO, H. CHEN and K. OKAMURA, *J. Ceram. Soc. Jpn* **100** (1992) 929.

Received 15 May
and accepted 28 August 1996